Scientific Research Publishing

Energy and Power Engineering, 2023, 15, 127-150
https://www.scirp.org/journal/epe
ISSN Online: 1947-3818
ISSN Print: 1949-243X

Minimization of Electric Power Losses on 132 kV and 220 kV Uganda Electricity Transmission Lines

Ounyesiga Living[1], Stephen Ndubuisi Nnamchi[2], Kelechi John Ukagwu[1], Abubakar Abdulkarim[3], Zaid Oluwadurotimi Jagun[4]

[1]Department of Electrical, Telecom and Computer Engineering, SEAS, Kampala International University, Kampala, Uganda
[2]Department of Mechanical Engineering, SEAS, Kampala International University, Kampala, Uganda
[3]Department of Electrical Engineering, Faculty of Engineering, Ahmadu Bello University, Zaria, Nigeria
[4]Department of Computer Engineering, Olabisi Onabanjo University, Ago-Iwoye, Nigeria
Email: living.ounyesiga@kiu.ac.ug, stephen.nnamchi@kiu.ac.ug, kelechi@kiu.ac.ug, aabulkarim@abu.edu.ng, Jagun.zaid@oouagoiwoye.edu.ng

How to cite this paper: Living, O., Nnamchi, S.N., Ukagwu, K.J., Abdulkarim, A. and Jagun, Z.O. (2023) Minimization of Electric Power Losses on 132 kV and 220 kV Uganda Electricity Transmission Lines. *Energy and Power Engineering*, **15**, 127-150.
https://doi.org/10.4236/epe.2023.152006

Received: January 7, 2023
Accepted: February 11, 2023
Published: February 14, 2023

Abstract

The classical minimization of power losses in transmission lines is dominated by artificial intelligence techniques, which do not guarantee global optimum amidst local minima. Revolutionary and evolutionary techniques are encumbered with sophisticated transformations, which weaken the techniques. Power loss minimization is crucial to the efficient design and operation of power transmission lines. Minimization of losses is one way to meet steady grid supply, especially at peak demand. Thus, this paper has presented a gradient technique to obtain optimal variables and values from the power loss model, which efficiently minimizes power losses by modifying the traditional power loss model that combines Ohm and Corona losses. Optimality tests showed that the unmodified model does not support the minimization of power losses on transmission lines as the Hessian matrix portrayed the maximization of power losses. However, the modified model is consistent with the gradient method of optimization, which yielded optimum variables and values from the power loss model developed in this study. The unmodified (modified) models for Bujagali-Kawanda 220 kV and Masaka West-Mbarara North 132 kV transmission lines in Uganda showed maximum power losses of 0.406 (0.391) and 0.452 (0.446) kW/km/phase respectively. These results indicate that the modified model is superior to the unmodified model in minimizing power losses in the transmission lines and should be implemented for the efficient design and operation of power transmission lines within and outside Uganda for the same transmission voltages.

Keywords

Minimization, Power Losses, Transmission Lines, Corona and Ohms Losses, Transmission Model

1. Introduction

Generating or converting electricity is quite difficult and requires a lot of time and resources. Thus, losing much of it is worrisome. For efficient performance of transmission lines, transmission losses should be highly minimized, this minimization of losses entails taking into account the equipment or material responsible for the losses, which is accounted for Ohms loss, whereas the environmental factors (air density, disruptive voltage) leading to loss of power in the transmission line is accounted by Corona loss. Power losses whether reactive or active could be curtailed at the design and testing stages [1] [2]. However, Ohms loss could be attributed to increased transmission current, the resistivity of the conducting materials, and the length of transmission lines [3]. Also decreasing the cross-section area of the conducting materials could also boost power losses in the transmission line [3] [4]. Further losses are known to be induced by the appreciable disparity between the phase and disruptive voltages, transmission frequency, and diameter (or radius) of the conducting materials [4] [5]. Conversely, decreasing air density increases losses due to environmental or weather conditions [7] [8].

Thus, transmission losses could be categorized into material losses; transmission equipment (capacitors and inductors in the transmission circuits), inherent losses (due to the nature of the current; thermal, electrical, and electromagnetic effects/atmospheric disasters [9] [10] [11]. These outrageous factors have to do with the inherent nature as part of the power is converted into heat and lost to the surroundings, and due to forceful earthling of the power by thunderstorms through the airs around the transmission lines as they lose their dielectric properties [7] [12]. However, the installation of thunder arresters could be a remedy or preventive measure [13] [14]. The use of aluminum (animal grades) is prone to power losses relative to copper which has better electrical and mechanical properties than aluminum. Equipment losses could be mitigated by minimizing reactive power in the transmission equipment and suppressing the magnitude of the eddy current developed in the inductors by designing the core of the inductor as laminates parallel to the magnetic field [15] [16] [17].

Notably, Non-gradient techniques of optimization—artificial intelligence methods. Patil *et al.* [18] presented Particle Swarm Optimization (PSO) and Salp Swarm Algorithm (SSA) techniques have been employed in finding optimum losses based on the active and reactive power losses; Monshizadeh *et al.* [19] recommended PSO as best algorithm for minimizing power loss in transmission lines; Baharozu *et al.* [20] improved PSO by choosing the load bus voltages, ge-

nerator active and reactive powers, line flow capacities as penalty functions in the objective function. PSO and IPSO-based optimal power flow solutions are compared with each other on IEEE 48, 118 and 300 bus systems [21]. It was found that the IPSO-based solution has fewer power losses than the PSO-based solution; Nadeem *et al.* [22] employed Compensators and Controllers in Flexible AC Transmission lines to minimize power losses. Naima *et al.* [23] and Kumar [24] combined genetic algorithm technology, and the particle swarm optimization in the western Algerian power system to reduce power losses in transmission lines; Kuru *et al.* [25] considered that Chaotic Artificial Bee Colony (CABC) Algorithm is more effective in minimizing active power losses than Artificial Bee Colony (ABC) Algorithm. CABC minimized up to 84,891 MW while ABC 86,203 MW; Nusair and Alomoush [26] and Jagun *et al.* [27] explored the Teaching Learning Based Optimization Algorithm (TLBO) technique for solving optimal reactive power dispatch and active power losses. TLBO has the efficiency to reduce the active power losses reasonably without violating any constraints, it also had excellent convergence compared to PSO-CM techniques; Badar *et al.* [28] employed the PSO algorithm with dynamic weights to minimize active power losses. The proposed technique showed better convergence and was better at reducing power losses compared to the existing techniques. The technique reduced losses from 11.61 MW to 8.7036 MW, which was a 25% reduction in total active power losses. Nevertheless, the optimization techniques based on artificial intelligence and deep neural network are widely employed in the minimization of power losses in the transmission lines, but are faced with problems of identifying the global minimum/maximum amidst minima/maxima.

However, the gradient method of minimizing power losses in the transmission line has the capacity to identify the global minimum/maximum. Pertinently, Bamigbola *et al.* [29] examined a flow model (mathematical Equation) to predict current and voltage parameters in the transmission lines, Revolutionized and simulated transmission model to obtain valid transmission losses; Sharma *et al.* [31], and Bisiriyu *et al.* [32] observe that Corona loss can be reduced by phase change in double circuit lines; Kuchanskyy and Zaitsev [33] [34] achieved loss minimization in transmission line through optimum length and radius of the transmission cable; Ali and Siddique [35] examined high Corona loss during wet or moisture in the atmosphere and low Corona loss in the dry atmosphere, degradation of the conducting material also causes Corona loss; Omeje [36] and Yaabari *et al.* [37] examined minimization of Corona loss at a very low transmission current and large spacing between bundled conductors; Llamo-Laborí and Santos-Fuentefria [38] observed that increase in spacing for the conductor bundles minimizes and balance Corona loss; Tonmitr *et al.* [6] conducted simulative research on minimizing the power losses using various conductor parameters, including conductor radius and system voltage; Ogar *et al.* [39] investigated distance between generating station, frequency and load center contributes to Corona loss based on Peek's formula and Peterson; Yahaya *et al.* [4] examined the

relationship between power losses from Corona and Corona characteristics using Matlab programs. Radio interference, audible noise, gaseous effluents, and shock potential are some of the impacts of Corona electrical surface gradients, and the performance of the conductor is influenced by conductor voltage, diameter and shape, dust, water drops, surface abnormalities like scratches; Al_issa *et al.* [40] used different approximation methods to examine active power loses through voltage and weather conditions; Al-Hamouz [41] and Hünnekens *et al.* [42] Compared Ohms and Corona loss under different loading conditions and found out that the percentage in moderate and light loadings could rise to 100% under deep Corona.

Notably, the application of the gradient method of optimization using the Corona and Ohms transmission loss model is not feasible as optimum variables of the objective function cannot be derived nor the optimum values possible. Expectantly, the gradient method of optimization guarantees global minimum/maximum. However, this could not be achieved using the traditional Corona and Ohms transmission loss model. Therefore, there is a silent need to develop Corona and Ohms models, which could be suitable for the gradient method of optimization in order to obtain the optimum objective function and optimum variables with the corresponding minimization values. Thus, this paper is concerned with the modification of the traditional power losses objective function by introducing a third dimensionally consistent term, a product of Corona and Ohms losses, and to validate the optimality of the unmodified and modified models on different power transmission lines.

2. Materials and Methods

This section presents the materials and methods used in this study.

2.1. Methodology

The methodology is detailed in the Sub-Sections 2.1.1 to 2.1.4 as follows:

2.1.1. Study Area

The study considered two transmission lines; Bujagali-Kawanda (B-K) transmission line (220 kV) and the Masaka West-Mbarara North (MW-MN) transmission line (220 kV) as shown in **Figure 1** and **Figure 2** respectively. This study was conducted on Uganda Electricity Transmission Lines where the two transmission lines were selected, Uganda is a landlocked country in East Africa, The country borders Kenya to the east, South Sudan to the north, the Democratic Republic of Congo to the west, Rwanda to the southwest, and Tanzania to the south. Geographically, Uganda is located close to the equator with latitude and longitude of 1.280˚N and 32.386˚E, respectively. Uganda covers a total area of 236,040 Km^2. This study covered two transmission lines of 132 kV (Masaka West-Mbarara North) and 220 kV (Bujagali-Kawanda) as shown in **Figure 1** and **Figure 2** respectively. Masaka West-Mbarara North transmission lines cover a route length of 130.5 km, five districts of Masaka, Kiruhura, Lyantonde, Lwengo and

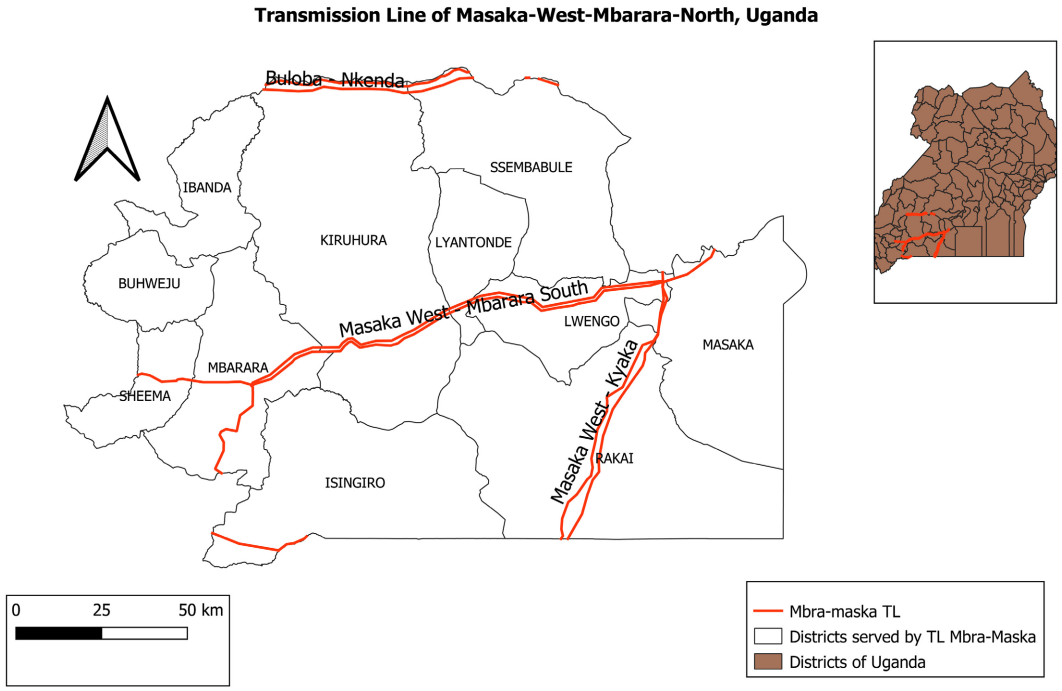

Figure 1. Map of the study area (Masaka West-Mbarara North) and the transmission lines.

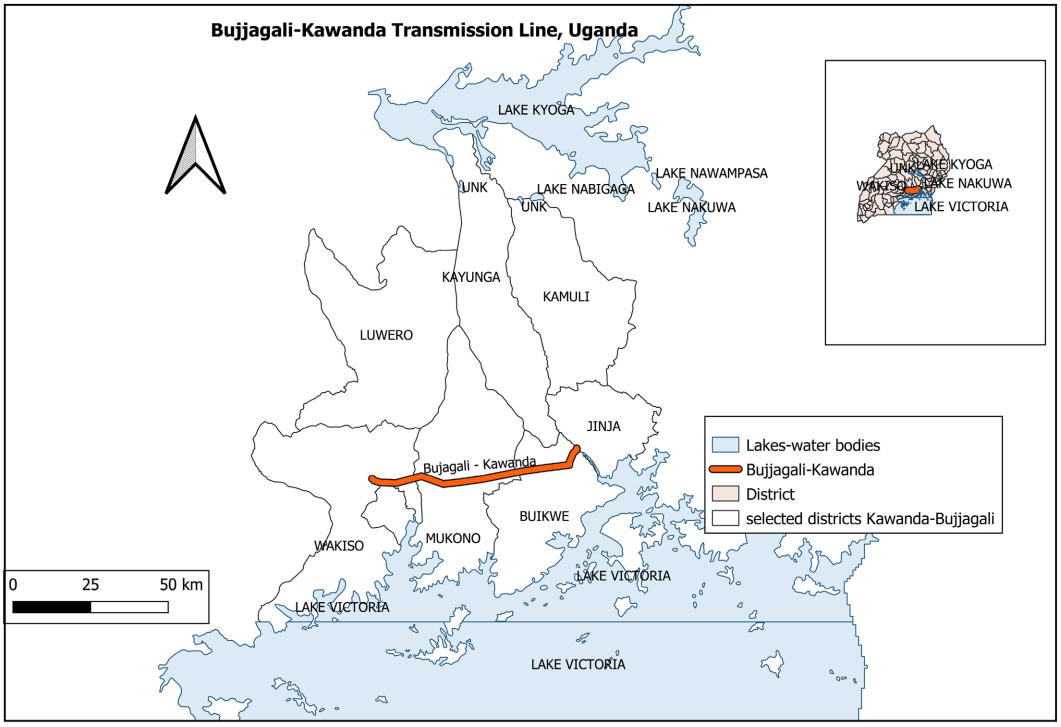

Figure 2. Map of the study area (Bujagali-Kawanda) and the transmission lines.

Masaka with a line rating of 151.6 MVA per circuit. Bujagali-Kawanda North transmission lines cover a route length of 84 km with a line rating of 205.8 MVA per circuit, which comprises four districts; Wakiso, Mukono, Buikwe and Jinja. Minimization of power losses in the transmission lines was carried out on both

lines of Masaka West-Mbarara North which is located at 0˚20'28.0"S, 31˚44'10.0"E (Latitude: −0.341; Longitude: 31.736) - 0˚36'25.776"S and 30˚39'16.211"E (Longitude: 30.655, Latitude: −0.607) respectively. Bujagali-Kawanda is located at 0.498˚N, 33.139˚E (Latitude: 0.495, Latitude 33.130˚) - latitude 0.422 and the longitude is: 32.542 respectively.

2.1.2. Methods

In the flow chart (Figure 3), the input variables for the unmodified power loss model (current (I), cross-section area (A), thermal resistivity (ρ), phase voltage (V), disruptive voltage (V_0), frequency (f), air density (γ), length (l), radius (r), spacing between conductors (d), radios (r), spacing between transmission lines (d) were identified from the literature. The modified model is obtained by adding the third term to the unmodified model in Equation (1), which is a product of a loss reduction factor (0.25) in Equation (2) and the square root of Ohm and Corona losses. Maple software was used to obtain the optimum variables based

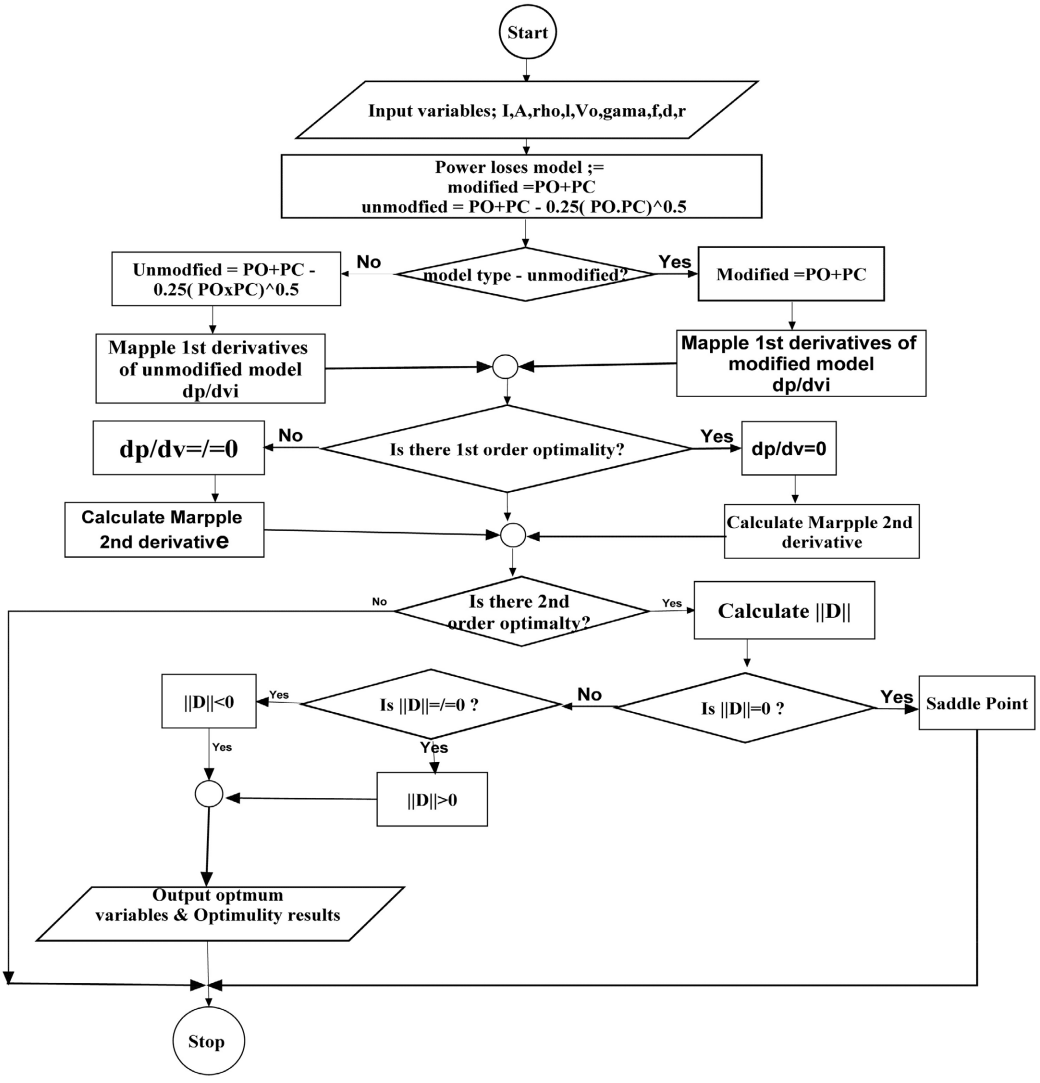

Figure 3. Flowchart for the minimization of power losses in the transmission lines.

on the first derivatives. The first derivative is further differentiated to obtain the second derivative, which forms the elements of the Hessian matrix. The determinant of the Hessian matrix is used to determine the optimality of power losses in the transmission lines. If the determinant is less than zero, implies minimization of power losses in the transmission lines, whereas a determinant greater than zero denotes maximization of power losses in the transmission lines. The optimum variables were used to calculate the optimum power losses in the transmission lines. The optimality test is implemented on the data acquired from the Uganda Electricity Transmission Company Limited [43]. Verification of the unmodified and modified models for minimization of power losses in the transmission lines was carried out with the transmission data acquired from [43].

2.1.3. Sources of Data and Collection

Input data used in the analysis is courtesy of the planning, design, operations, and maintenance department of [43]. The following transmission data from [43]; voltage, current, frequency, conductor dimensions, spacing of conductors, thermal and electrical characteristics of the conductor for the transmission lines (132 kV (Masaka West-Mbarara North) and 220 kV (Bujagali-Kawanda) were used in the analysis.

2.1.4. Data Analysis Techniques

The data obtained from [43] were imputed into Maple-derived models to calculate; the optimum values of the optimum variables, and second-order derivatives of these variables. These results were exported to a Microsoft Excel spreadsheet to calculate the determinant of the Hessian matrix (matrix of second-order derivatives). The determinate of the Hessian matrix served as a criterion for the optimality test and decision. Also, a Spread sheet of power losses was developed in a Microsoft Excel spreadsheet as a function of current and voltages in the transmission lines. Furthermore, the spreadsheet power losses were exported to Origin (7.0) to obtain three dimensional (3D) plot of current, voltage and power losses in the transmission lines. The analysis was conducted for both unmodified and modified transmission power loss models to show the robustness of the modified model. **Figure 3** portrays the algorithm or the flowchart of the analysis.

2.2. Formulation of Power Losses in Transmission Lines

Total transmission power losses are defined by Ohms and Corona losses [30] in Equation (1). Supposedly, Equation (1) minimizes total losses on the transmission lines via the Hessian matrix with a determinant above zero. Equation (1) serves an objective function for the minimization of power losses, p in the transmission line depends on the uncoupled (individual) losses in Equation (1).

$$p = p_O + p_C \tag{1}$$

where p_O (W/km/Phase) is the Ohms loss and p_C (W/km/Phase) is the Corona loss.

Equation (1) is fully defined in Equation (2)

$$p = \frac{I^2\rho}{A} + 242\times10^{-05}\left(V - V_O\right)^2\left(\frac{f+25}{\gamma l}\right)\left(\frac{r}{d}\right)^{0.5}\left(\text{W/km/phase}\right) \tag{2}$$

where I(A or C/s) is the transmission current, ρ(Ωm) is the resistivity of the transmission cable, l(m) is the length of the transmission line, A(m^2) is cross-section area, V(V) is the phase voltage, V_0(V) is the disruptive voltage, f(Hz) is the transmission frequency, γ(kg/m^3) air density factor, r(m) is the radius of the transmission lines, d(m) is space between transmission lines.

Applying Equation (2) as an objective function for minimizing power losses on the transmission lines, the optimum variables (I^*, V^*, γ^*) cannot be established. Thus, the need to establish a modified objective function to obtain the optimum variables and to minimize transmission power losses in Equation (3). Equation (3) is made up of uncoupled (individual) and coupled (combined) losses

$$p = p_O + p_C - 0.25\left(p_O p_C\right)^{0.5} \tag{3}$$

Equation (3) can be presented in Equation (4), that is

$$\begin{aligned}\tilde{p} = {} & \frac{I^2\rho}{A} + 242\times10^{-5}\left(V - V_0\right)^2\left(\frac{f+25}{\gamma l}\right)\left(\frac{r}{d}\right)^{0.5} \\ & - 0.25\left[\left(\frac{I^2\rho}{A}\right)\left(242\times10^{-5}\left(V - V_0\right)^2\left(\frac{f+25}{\gamma l}\right)\left(\frac{r}{d}\right)^{0.5}\right)\right]^{0.5}\left(\text{kW/km/phase}\right)\end{aligned} \tag{4}$$

The optimum transmission variables ($I^*, V^*, V_0^*, \gamma^*$) are presented in the supplementary file (**Appendix**).

2.2.1. Proof of Optimality of the Objective Function-Transmission Losses

The objective function could be proved to be either maximum or minimum by obtaining the matrix of second order derivative of the objective function from Equation (4) in Equation (5) Hessian matrix, H

$$H = \begin{bmatrix} \frac{\partial^2(\tilde{p})}{\partial^2 I^2} & \frac{\partial^2(\tilde{p})}{\partial I \partial V} & \frac{\partial^2(\tilde{p})}{\partial I \partial \gamma} \\ \frac{\partial^2(\tilde{p})}{\partial V \partial I} & \frac{\partial^2(\tilde{p})}{\partial^2 V^2} & \frac{\partial^2(\tilde{p})}{\partial V \partial \gamma} \\ \frac{\partial^2(\tilde{p})}{\partial \gamma \partial I} & \frac{\partial^2(\tilde{p})}{\partial \gamma \partial V} & \frac{\partial^2(\tilde{p})}{\partial^2 \gamma^2} \end{bmatrix} \tag{5}$$

2.2.2. Derivatives of the Hessian Matrix

The derivatives of Hessian matrix are found in the **Appendix**. Applying Equations (1) and (2) as an objective function for minimizing power losses on the transmission lines, the optimum variables ($I^*, V^*, V_0^*, \gamma^*, d^*$) cannot be established. Thus, the need to establish a modified objective function to obtain the optimum variables and to minimize transmission power losses in Equation (3). Equation (3) comprises of uncoupled (individual) and coupled (combined)

losses.

The determinant (D) of the unmodified Hessian matrix in Equation (5) is given in Equation (6) for 132 kV (Masaka West-Mbarara North)

$$D = \begin{bmatrix} 2\rho/A & 0 & 0 \\ 0 & \dfrac{121(f+25)\sqrt{r/d}}{25000\gamma l} & -\dfrac{121(f+25)(V-V_0)\sqrt{r/d}}{25000\gamma^2 l} \\ 0 & -\dfrac{121(f+25)(V-V_0)\sqrt{r/d}}{25000\gamma^2 l} & \dfrac{121(f+25)(V-V_0)^2\sqrt{r/d}}{25000\gamma^3 l} \end{bmatrix} \quad (6)$$

$$= \begin{bmatrix} 0.000166 & 0 & 0 \\ 0 & 6.486\times10^{-8} & -0.000932 \\ 0 & -0.000932 & 13.397 \end{bmatrix}$$

The determinant (D) of modified Hessian matrix in Equation (5) is given in Equation (7) for 132 kV (Masaka West-Mbarara North)

$$D = \begin{bmatrix} \text{Eq.}(9) & \text{Eq.}(12) & \text{Eq.}(13) \\ \text{Eq.}(15) & \text{Eq.}(10) & \text{Eq.}(14) \\ \text{Eq.}(16) & \text{Eq.}(17) & \text{Eq.}(11) \end{bmatrix}$$

$$= \begin{bmatrix} 0.000166 & -4.0971\times10^{-7} & 0.00294 \\ -4.0971\times10^{-7} & 6.486\times10^{-8} & -0.0009 \\ 0.00294 & -0.000904 & 12.783 \end{bmatrix} \quad (7)$$

The determinant (D) of Unmodified Hessian matrix in Equation (5) is given in Equation (8) for 220 kV (Bujagali-Kawanda)

$$\begin{bmatrix} 2\rho/A & 0 & 0 \\ 0 & \dfrac{121(f+25)\sqrt{r/d}}{25000\gamma l} & -\dfrac{121(f+25)(V-V_0)\sqrt{r/d}}{25000\gamma^2 l} \\ 0 & -\dfrac{121(f+25)(V-V_0)\sqrt{r/d}}{25000\gamma^2 l} & \dfrac{121(f+25)(V-V_0)^2\sqrt{r/d}}{25000\gamma^3 l} \end{bmatrix} \quad (8)$$

$$= \begin{bmatrix} 0.000339 & 0 & 0 \\ 0 & 4.771\times10^{-8} & -0.00432 \\ 0 & -0.00432 & 391.716 \end{bmatrix}$$

The determinant (D) of modified Hessian matrix in Equation (5) is given in Equation (9) for 220 kV (Bujagali-Kawanda)

$$D = \begin{bmatrix} \text{Eq.}(14) & \text{Eq.}(17) & \text{Eq.}(18) \\ \text{Eq.}(20) & \text{Eq.}(15) & \text{Eq.}(19) \\ \text{Eq.}(21) & \text{Eq.}(22) & \text{Eq.}(16) \end{bmatrix}$$

$$= \begin{bmatrix} 0.000339 & -5.0245E\times10^{-7} & 0.0228 \\ -5.0245\times10^{-7} & 4.771\times10^{-8} & -0.00409 \\ 0.0228 & 0.00427 & 383.773 \end{bmatrix} \quad (9)$$

3. Results and Discussion

The tables and figures resulting from the study are presented in this section. The

explanation of the tables and figures from the results is follows.

3.1. Presentation of Results

Table 1 gives the summary of input data used for the analysis of 132 kV transmission lines, whereas Table 2 provides the input data employed in the analysis of 220 kV transmission lines. Table 3 contains the Hessian matrix optimality tests results. Figure 4 describes power losses in Bujagali-Kawanda transmission line, Figure 5 portrays power losses in Masaka West-Mbarara North transmission line, Figure 6 explains power losses in Bujagali-Kawanda transmission line, whereas Figure 7 shows power losses in Masaka West-Mbarara North transmission line. Figure 8 presents power losses in the Bujagali-Kawanda transmission

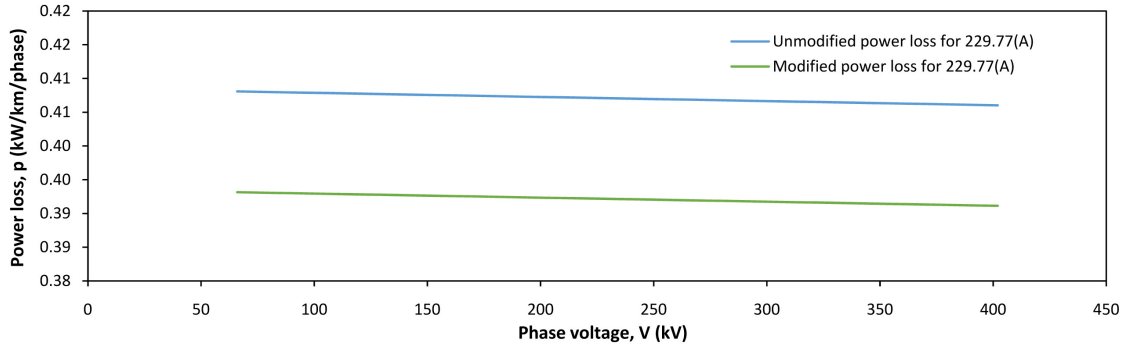

Figure 4. Power losses in Bujagali-Kawanda transmission line.

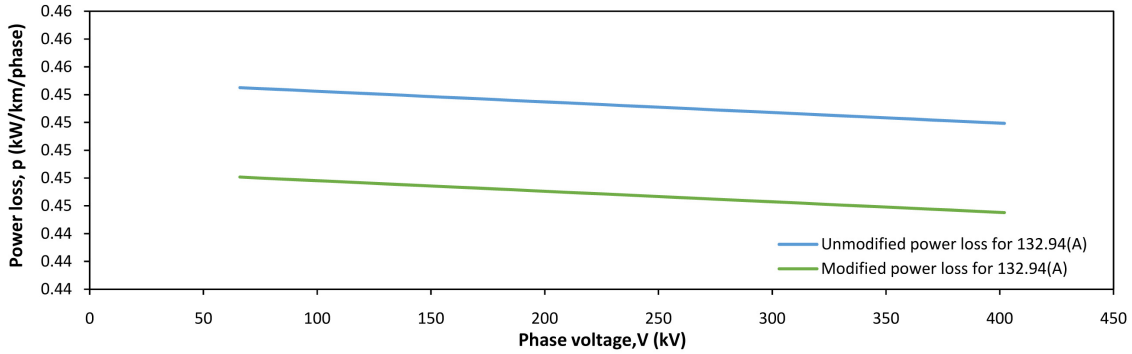

Figure 5. Power losses in Masaka West-Mbarara North transmission line.

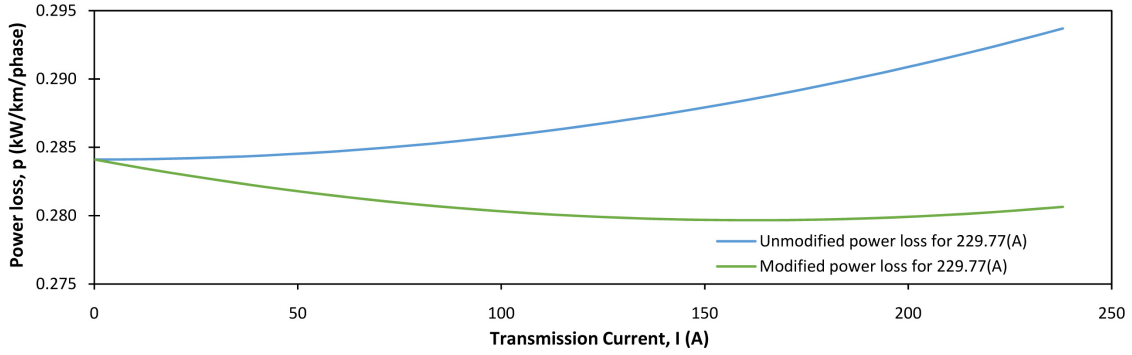

Figure 6. Power losses in Bujagali-Kawanda transmission line.

Table 1. Input data for the optimization of power losses in the transmission lines (UETCL, 2022).

S#	Parameters	Symbol	132 kV (Masaka West-Mbarara North)	220 kV (Bujagali-Kawanda)
1.	Transmission current (A)	I	132.94	229.77
2.	Resistivity of transmission cable	ρ	2.65×10^{-8}	2.65×10^{-8}
3.	Length of transmission line (km)	l	130.5	130.5
4.	Cross-section area	A	0.00032	0.000157
5.	Phase voltage	V	132	220
6.	Disruptive voltage	V_0	88.409	94.555
7.	Transmission frequency	f	50.09	50.09
8.	Air density factor	γ	1.00433	1.00433
9.	Radius of transmission cable (30/3.71mm ≡ 30/0.00371 m)	r	0.00186	0.0013
10.	Spacing between the transmission cables (m)	d	3.740	4.540

Table 2. Optimization results of power losses in the transmission lines based on modified and unmodified models.

S#	Parameters	Symbol	Unmodified model		Modified model	
			132 kV (Masaka West-Mbarara North)	220 kV (Bujagali-Kawanda)	132 kV (Masaka West-Mbarara North)	220 kV (Bujagali-Kawanda)
1.	Transmission current (A)	I^*	NA	NA	33.994	132.791
2.	Resistivity of transmission cable	ρ^*	NA	NA	NA	NA
3.	Length of transmission line (m)	l^*	NA	NA	NA	NA
4.	Cross-section area (m^2)	A^*	NA	NA	NA	NA
5.	Phase voltage (kV)	V^*	NA	NA	119.0972	132.918
6.	Disruptive voltage (kV)	V_0^*	NA	NA	NA	NA
7.	Transmission frequency	f^*	NA	NA	NA	NA
8.	Air density factor	γ^*	NA	NA	1.255	1.469
9.	Radius of transmission cable (30/3.71 mm ≡ 30/0.00371 m)	r^*	NA	NA	NA	NA
10.	Space between transmission cable (m)	d^*	NA	NA	NA	NA

NA: Not Available.

line as a function of air density. Similarly, Figure 9 describes power losses in the Masaka West-Mbarara North transmission line as a function of air density. Lastly, Figure 10(a) and Figure 10(b) show the unmodified and modified 3-D plots of power losses on 220 kV-Kawana transmission lines. Likewise, Figure 11(a) and Figure 11(b) show the unmodified and modified 3-D plot of power losses on 220 kV Masaka West-Mbarara North transmission lines.

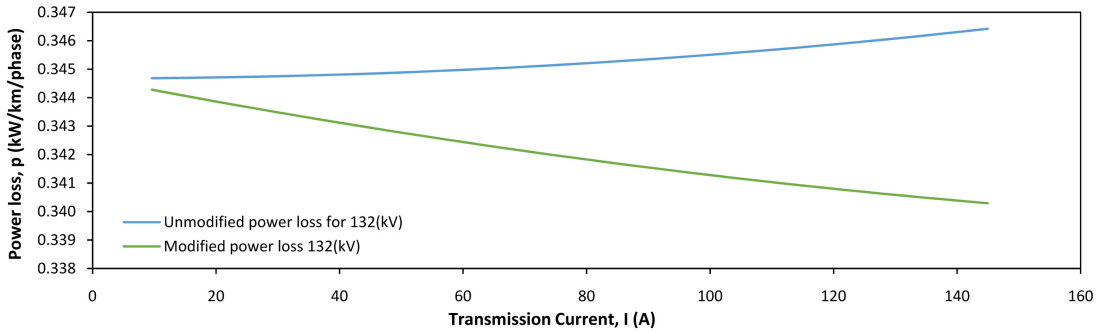

Figure 7. Power losses in Masaka West-Mbarara North transmission line.

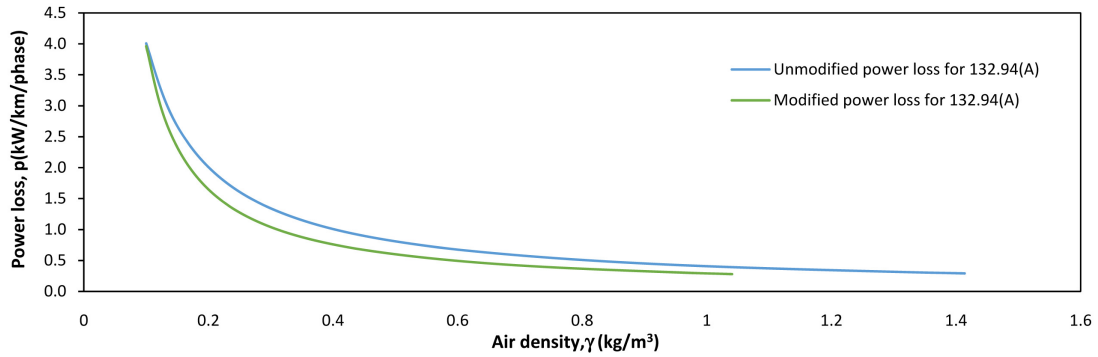

Figure 8. Power losses in Bujagali-Kawanda transmission line as a function of air density.

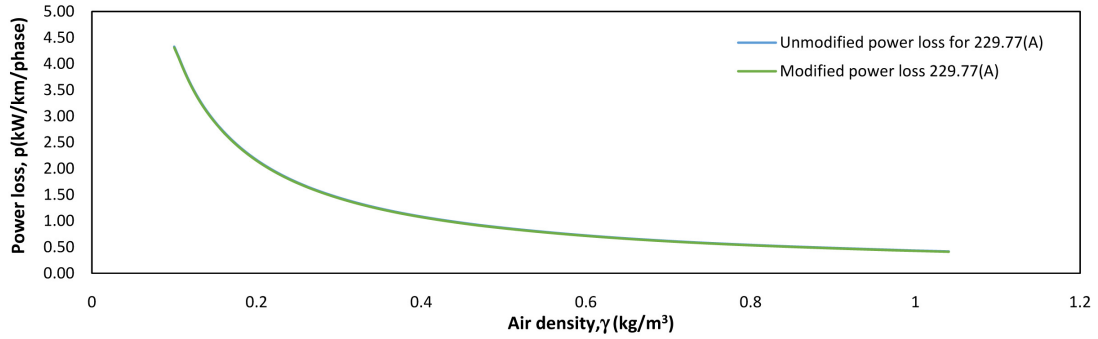

Figure 9. Power losses in Masaka West-Mbarara North transmission line as a function of air density.

Table 3. Optimality tests based on the Hessian matrix in Equation (8)

S#	Transmission Line	Equation Number		Value	Model type	Remarks
		Hessian	Determinant	Determinant Hessian		
1.	132 kV (Masaka West-Mbarara North)	Equation (8)	Equation (18)	-1.573×10^{-19}	Unmodified	Maximization ($D < 0$)
2.	132 kV (Masaka West-Mbarara North)	Equation (8)	Equation (19)	1.536×10^{-12}	Modified	Minimization ($D > 0$)
3.	220 kV (Bujagali-Kawanda)	Equation (8)	Equation (20)	$-6.765\text{E} \times 10^{-18}$	Unmodified	Maximization ($D < 0$)
4.	220 kV (Bujagali-Kawanda)	Equation (8)	Equation (21)	1.757×10^{-11}	Modified	Minimization ($D > 0$)

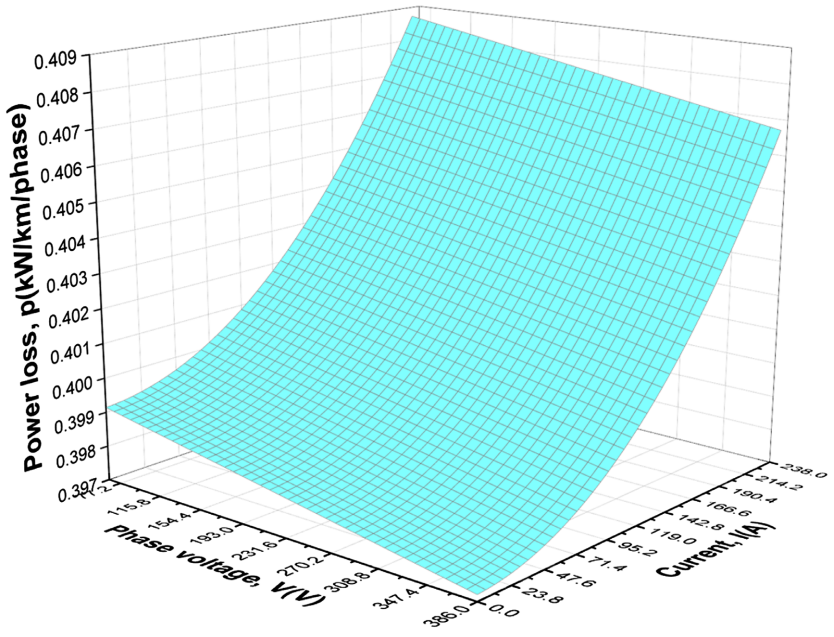

(a)

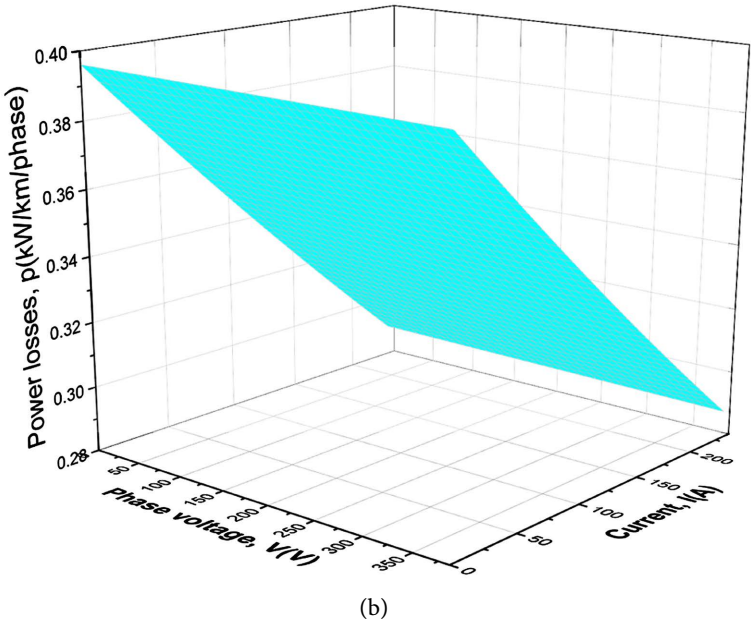

(b)

Figure 10. (a) Unmodified 3-D plot of power losses for 220 kV Bujagali-Kawana transmission line; (b) Modified 3-D plot of power losses on 220 kV Bujagali-Kawana transmission line.

3.2. Discussion of Results

3.2.1. Results of Unmodified and Modified Models

Table 1 presents the Input data for the optimization of power losses on 132 kV (Masaka West-Mbarara North) and 220 kV (Bujagali-Kawanda) transmission lines. These parameters were used to obtain optimum values for both modified and unmodified models as shown in Table 2. It was observed that for the unmodified model, there were no optimum variables nor values obtained for both

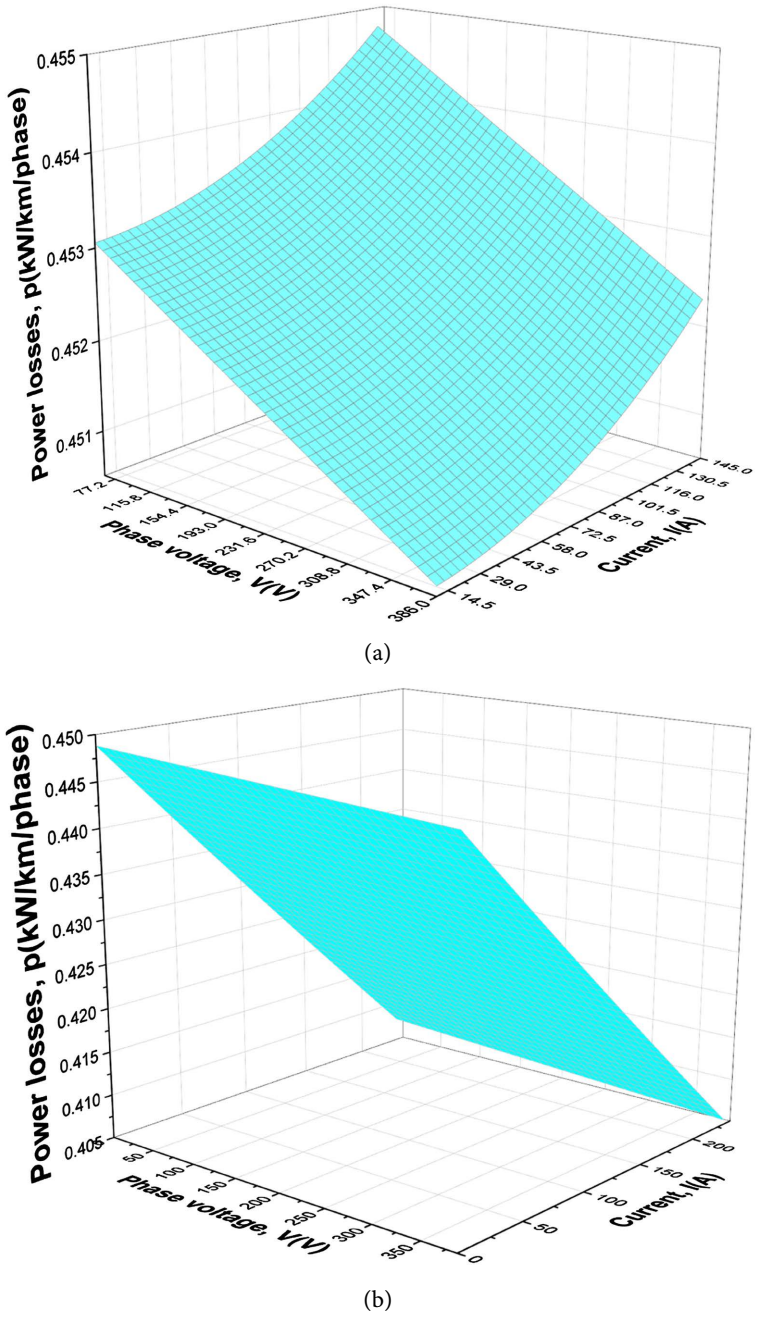

Figure 11. (a) Unmodified 3-D plot of power losses for 132 kV Masaka West-Mbarara North transmission line; (b) Modified 3-D plot of power losses for 132 kV Masaka West-Mbarara North transmission line.

transmission lines because the model could not yield optimal variables. However, the modified model on 132 kV (Masaka West-Mbarara North) transmission line optimum variables and values were obtained [29] as a result of power loss penalty function introduced in the traditional power loss model; the optimum transmission current (33.995 A), Phase voltage (119.0972 V), and air density (1.255 kg/m^3) minimized power loss in the transmission line; and on 220 kV (Bujagali-Kawanda) transmission line optimum variables and values were estab-

lished, transmission current (132.7905080 A), Phase voltage (132.918 V) and air density (1.469 kg/m^3), which minimize power losses. Table 3 presents optimality tests based on the Hessian matrix. It is observed that both 132 kV (Masaka West-Mbarara North) and 220 kV (Bujagali-Kawanda) transmission lines under an unmodified model maximized power losses as the determinant is less than zero ($D < 0$), -1.573×10^{-19} and $-6.765\text{E} \times 10^{-18}$, respectively. It is also observed that 132 kV (Masaka West-Mbarara North) and 220 kV (Bujagali-Kawanda) transmission lines under the modified model supported minimization of power losses as the determinant of Hessian matrix is greater than zero ($D > 0$), 1.536×10^{-12} and 1.757×10^{-11} respectively.

3.2.2. Discussion of Power Losses in the Transmission Lines

Figure 4 shows the power losses plotted against the phase voltage of the Bujagali-Kawanda transmission line plotted for both modified and unmodified models. The graphs show the voltage range: 66 to 402 kV, the losses in unmodified and modified models ranged (0.408 - 0.406 kW/km/phase) and (0.393 - 0.391 kW/km/phase) respectively. This shows that the modified model minimized power losses due to the implementation of optimum variables and values.

Figure 5 presents the input data for power losses plotted against the phase voltage of the Masaka West-Mbarara North transmission line plotted for both modified and unmodified models. The graphs show the voltage range: 66 to 402 kV, the losses in the unmodified and modified models ranged (0.455 - 0.452 kW/km/phase) and (0.448 - 0.446 kW/km/phase) respectively. This shows that the modified model minimized power losses due to the implementation of optimum variables, values, and the virtue of the third term (presence of power loss penalty function) incorporated in the modified model.

Observation in Figure 6 indicates that both models at low transmission current have no disparity but at high transmission current because ohmic losses is weak, there is a quite appreciable difference because ohmic effect is strong. This implies that the modified model has a high potential to minimize power loss relative to the unmodified model. The graphs show the transmission current ranged from 24 A to 238 A, and the losses in unmodified and modified models ranged (0.284 - 0.294 kW/km/phase) and (0.283 - 0.281 kW/km/phase) respectively.

Figure 7 presents the input data for power losses plotted against the phase transmission current of the Masaka West-Mbarara North transmission lines plotted for both modified and unmodified models. The graph shows the transmission current range: 13 to 145 A, the losses in unmodified and modified models ranged (0.345 - 0.347 kW/km/phase) and (0.344 - 0.340 kW/km/phase) respectively. This shows that the modified model minimized power losses when compared with the unmodified model due to presence of power loss penalty function [29].

Furthermore, Figure 7 presents the power losses plotted against the air density of the Bujagali-Kawanda transmission line plotted for both modified and un-

modified models. The graph obtained shows that the results support or identify the modified model as an effective one in minimizing power losses and this means the power losses are attributed to both Corona and Ohms losses are effectively minimized.

In addition, Figure 9 shows an inappreciable discrepancy in the transmission power losses by unmodified and modified models, this means that the atmosphere in the transmission lines is uniform and could not support any meaningful difference in power losses for the unmodified and modified models because air factor contribution to power losses is minimal relative to other transmission variables.

Figure 10(a) and Figure 10(b) show the three-dimensional graph of power losses, phase voltage, and current for the 220 kV Bujagali-Kawana transmission lines. The power losses for both unmodified and modified are 0.305 and 0.288 kV/km/phase respectively as shown in Figure 11(a) and Figure 11(b). For the 132 kV Masaka West-Mbarara North transmission lines. The power losses for both unmodified and modified are 0.302 and 0.289 kV/km/phase respectively as presented in Figure 11(a) and Figure 11(b) which implies that the modified has a high potential for power loss minimization in both transmission lines engendered by the power loss penalty function or power loss modification term.

3.2.3. Optimality Test

The Hessian matrix was used to carry out optimality test for both modified and unmodified models. It is observed that both 132 kV (Masaka West-Mbarara North) and 220 kV (Bujagali-Kawanda) transmission lines under an unmodified model maximized power losses as $D < 0$, -1.573×10^{-19} and -6.765×10^{-18} respectively, as it lacks optimum variables and values. It is also observed that for both 132 kV (Masaka West-Mbarara North) and 220 kV (Bujagali-Kawanda) transmission lines under the modified model minimized power losses as $D > 0$, 1.536×10^{-12} and 1.757×10^{-11} respectively, since it has both optimum variables and values.

4. Conclusion

A modified model for power loss minimization in the transmission lines of Bujagali-Kawanda and Masaka West-Mbarara North in Uganda has been developed. The optimum variables and values of transmission current, phase voltage and air density were determined using the gradient optimization technique that is the first derivative of the modified model and is feasible with the modified model. An optimality test was also carried out using Hessian matrix both on the unmodified and modified models. The optimal results for both modified and unmodified established that the modified model has a high potential to minimize power losses in the transmission lines. Consequently, this paper recommends that a modified model should be implemented in the transmission line in the design and operation of transmission lines, due to its ability to minimize power losses in the transmission lines. The results of this study are not limited peculiar

to Uganda Electricity Transmission Lines, they could be implemented by other transmission lines outside Uganda.

Acknowledgements

The authors wish to acknowledge Uganda Electricity Transmission Lines for availing input data used in the analysis of the local transmission lines.

Conflicts of Interest

No conflict of interest of any kind.

References

[1] Jenkins, N. and Thornycroft, J. (2018) Grid Connection of Photovoltaic Systems: Technical and Regulatory Issues. In: *McEvoy's Handbook of Photovoltaics*, Academic Press, Cambridge, 847-876. https://doi.org/10.1016/B978-0-12-809921-6.00022-7

[2] Maza-Ortega, J.M., Acha, E., García, S. and Gómez-Expósito, A. (2017) Overview of Power Electronics Technology and Applications in Power Generation Transmission and Distribution. *Journal of Modern Power Systems and Clean Energy*, **5**, 499-514. https://doi.org/10.1007/s40565-017-0308-x

[3] Wain-Martin, A., Campana, R., Morán-Ruiz, A., *et al.* (2020) Synthesis and Processing of SOFC Components for the Fabrication and Characterization of Anode Supported Cells. *Boletín de la Sociedad Española de Cerámica y Vidrio*, **61**, 264-274. https://doi.org/10.1016/j.bsecv.2020.11.008

[4] Yahaya, E.A., Jacob, T., Nwohu, M.N. and Sadiq, A.A. (2013) Power Loss Due to Corona on High Voltage Transmission Lines. *IOSR Journal of Electrical and Electronics Engineering*, **8**, 14-19. https://doi.org/10.9790/1676-0831419

[5] Tonmitr, K. and Ratanabuntha, T. (2016) Comparison of Power Loss Due to Corona Phenomena Model with Peek's Formula in High Voltage 115 kV and 230 kV System. *Procedia Computer Science*, **86**, 385-388. https://doi.org/10.1016/j.procs.2016.05.037

[6] Tonmitr, K., Ratanabuntha, T., Tonmitr, N. and Kaneko, E. (2016) Reduction of Power Loss from Corona Phenomena in High Voltage Transmission Line 115 and 230 kV. *Procedia Computer Science*, **86**, 381-384. https://doi.org/10.1016/j.procs.2016.05.108

[7] Saleem, M.Z., Kamran, M., Amin, S. and Ullah, R. (2020) Investigation on Dielectric Properties of Chlorodifluoromethane and Mixture with Other N2/CO_2/Air as a Promising Substitute to SF6 in High Voltage Application. *Electrical Engineering*, **102**, 2341-2348. https://doi.org/10.1007/s00202-020-01034-2 https://www.springerprofessional.de/en/investigation-on-dielectric-properties-of-chlorodifluoromethane-/18080998

[8] Jorge, R.S. and Hertwich, E.G. (2013) Environmental Evaluation of Power Transmission in Norway. *Applied Energy*, **101**, 513-520. https://doi.org/10.1016/j.apenergy.2012.06.004

[9] Mahdy, A.M., Lotfy, K., Ahmed, M.H., *et al.* (2020) Electromagnetic Hall Current Effect and Fractional Heat Order for Microtemperature Photo-Excited Semiconductor Medium with Laser Pulses. *Results in Physics*, **17**, Article ID: 103161. https://doi.org/10.1016/j.rinp.2020.103161

[10] Waseem, M. and Manshadi, S.D. (2020) Electricity Grid Resilience amid Various

Natural Disasters: Challenges and Solutions. *The Electricity Journal*, **33**, Article ID: 106864. https://doi.org/10.1016/j.tej.2020.106864

[11] Sathaye, J.A., Dale, L.L., Larsen, P.H., *et al.* (2013) Estimating Impacts of Warming Temperatures on California's Electricity System. *Global Environmental Change*, **23**, 499-511. https://doi.org/10.1016/j.gloenvcha.2012.12.005

[12] Lalbakhsh, A., Simorangkir, R.B., Bayat-Makou, N., *et al.* (2022) Advancements and Artificial Intelligence Approaches in Antennas for Environmental Sensing. In: Asadnia, M., Razmjou, A. and Beheshti, A., Eds., *Artificial Intelligence and Data Science in Environmental Sensing*, Elsevier, Amsterdam, 19-38. https://www.elsevier.com/books/artificial-intelligence-and-data-science-in-environmental-sensing/asadnia/978-0-323-90508-4 https://doi.org/10.1016/B978-0-323-90508-4.00004-6

[13] Shariatinasab, R. and Gholinezhad, J. (2017) The Effect of Grounding System Modeling on Lightning-Related Studies of Transmission Lines. *Journal of Applied Research and Technology*, **15**, 545-554. https://doi.org/10.1016/j.jart.2017.06.003

[14] Pourakbari-Kasmaei, M. and Lehtonen, M. (2020) Enhancing the Protective Performance of Surge Arresters against Indirect Lightning Strikes via an Inductor-Based Filter. *Energies*, **13**, 4754. https://doi.org/10.3390/en13184754

[15] Doychinov, Y. Research of the Didactic Features in the Game Design Education. Sessions Schedule & Abstracts Програма & Резюмета. 125. https://scholar.google.com/citations?user=OqPzw4UAAAAJ&hl=bg

[16] Du Plessis, A., MacDonald, E., Waller, J.M. and Berto, F. (2021) Non-Destructive Testing of Parts Produced by Laser Powder Bed Fusion. In: *Fundamentals of Laser Powder Bed Fusion of Metals*, Elsevier, Amsterdam, 277-300. https://www.elsevier.com/books/fundamentals-of-laser-powder-bed-fusion-of-metals/yadroitsev/978-0-12-824090-8 https://doi.org/10.1016/B978-0-12-824090-8.00016-0

[17] Yamaguchi, M., Suezawa, K., Takahashi, Y., *et al.* (2000) Magnetic Thin-Film Inductors for RF-Integrated Circuits. *Journal of Magnetism and Magnetic Materials*, **215**, 807-810. https://doi.org/10.1016/S0304-8853(00)00293-6

[18] Patil, N., Vijay, K.E. and Kulkarni, G.A. (2020) Power Losses Minimization in Transmission System Using Particle Swarm Optimization and Salp Swarm Algorithm. *European Journal of Molecular and Clinical Medicine*, **7**, 2020. https://ejmcm.com/article_1818.html

[19] Monshizadeh, S., Uhlen, K. and Hegglid, G.J. (2020) Transmission Loss Minimization Using Artificial Intelligent Algorithm for Nordic44 Network Model Based on Hourly Load Variation. *IFAC-PapersOnLine*, **53**, 13254-13261. https://doi.org/10.1016/j.ifacol.2020.12.154

[20] Baharozu, E., Soykan, G., Altay, O. and Kalenderli, O. (2015) An Improved Particle Swarm Optimization Method to Optimal Reactive Power Flow Problems. 2015 9*th International Conference on Electrical and Electronics Engineering* (*ELECO*), Bursa, 26-28 November 2015, 991-995. https://doi.org/10.1109/ELECO.2015.7394600

[21] Olorunfemi, T.R. and Nwulu, N.A. (2020) Review of Mathematical Optimization Applications in Renewable Energy-Powered Microgrids. In: *Advances in Manufacturing Engineering*, Springer, Singapore, 603-613. https://doi.org/10.1007/978-981-15-5753-8_55

[22] Nadeem, M., Imran, K., Khattak, A., *et al.* (2020) Optimal Placement, Sizing and Coordination of FACTS Devices in Transmission Network Using Whale Optimization Algorithm. *Energies*, **13**, 753. https://doi.org/10.3390/en13030753

[23] Naima, K., Fadela, B., Imene, C. and Abdelkader, C. (2015) Use of Genitic Algorithm and Particle Swarm Optimisation Methods for the Optimal Control of the Reactive Power in Western Algerian Power System. *Energy Procedia*, **74**, 265-272. https://doi.org/10.1016/j.egypro.2015.07.597

[24] Kumar, A.S. (2013) Corona Effect on Transmission Lines. *International Journal of Electrical and Electronics Engineering Research* (*IJEEER*), **3**, 133-136. https://www.ijser.org/researchpaper/Effect-of-Corona-on-Transmission-Lines-due-to-its-linked-Parameters.pdf

[25] Kuru, L., Ozturk, A., Kuru, E. and Cobanli, S. (2016) Smanjenje gubitka aktivne snage u elektro-energetskim sustavima primjenom algoritma kaotične umjetne kolonije pčela. *Tehnički Vjesnik*, **23**, 491-498.

[26] Nusair, K.N. and Alomoush, M.I. (2017) Optimal Reactive Power Dispatch Using Teaching Learning Based Optimization Algorithm with Consideration of FACTS Device "STATCOM". 2017 10*th Jordanian International Electrical and Electronics Engineering Conference* (*JIEEEC*), Amman, 16-17 May 2017, 1-12. https://doi.org/10.1109/JIEEEC.2017.8051398

[27] Jagun, Z.O., Olajide, M.B., Wokoma, B.A. and Osegi, E.N. (2021) Power Loss Minimization Load Flow Studies Using Artificial Bee Colony Swarm Intelligence Technique. *Nigerian Journal of Technology*, **40**, 728-731. https://doi.org/10.4314/njt.v40i4.19

[28] Badar, A.Q., Umre, B.S. and Junghare, A.S. (2012) Reactive Power Control Using Dynamic Particle Swarm Optimization for Real Power Loss Minimization. *International Journal of Electrical Power & Energy Systems*, **41**, 133-136. https://doi.org/10.1016/j.ijepes.2012.03.030

[29] Bamigbola, O.M., Ali, M.M. and Awodele, K.O. (2014) Predictive Models of Current, Voltage, and Power Losses on Electric Transmission Lines. *Journal of Applied Mathematics*, **2014**, Article ID: 146937. https://doi.org/10.1155/2014/146937

[30] Bamigbola, O.M., Ali, M.M. and Oke, M.O. (2014) Mathematical Modeling of Electric Power Flow and the Minimization of Power Losses on Transmission Lines. *Applied Mathematics and Computation*, **241**, 214-221. https://doi.org/10.1016/j.amc.2014.05.039

[31] Sharma, S., Goel, K., Gupta, A. and Kumar, H. (2012) Corona Effects on eHv AC Transmission Lines. *International Journal of Scientific Research Engineering & Technology*, **1**, 160-164.

[32] Bisiriyu, A.O., Ajetunmobi, E.O., Omotayo, M.E. and Adeshola, M. (2017) Analysis of Corona Loss on the Nigerian 28-Bus, 330 kV Transmission Grid. *International Journal of Science and Research* (*IJSR*), **6**, 2009-2011. https://doi.org/10.21275/ART20175355

[33] Kuchanskyy, V. and Zaitsev, I.O. (2020) Corona Discharge Power Losses Measurement Systems in Extra High Voltage Transmissions Lines. 2020 *IEEE 7th International Conference on Energy Smart Systems* (*ESS*), Kyiv, 12-14 May 2020, 48-53. https://doi.org/10.1109/ESS50319.2020.9160088

[34] Simeon, M., Tita, W.S., Adejumobi, I.A. and Elizabeth, A. (2018) Minimization of Active Transmission Loss in Power Systems Using Static Var Compensator. *International Journal of Applied Engineering Research*, **13**, 4951-4959. https://www.ripublication.com/ijaer18/ijaerv13n7_47.pdf

[35] Ali, B. and Siddique, I. (2016) Effect of Corona on Transmission Lines Due to Its Linked Parameters. *International Journal of Scientific & Engineering Research*, **7**, 581-583.

https://www.ijser.org/researchpaper/Effect-of-Corona-on-Transmission-Lines-due-to-its-linked-Parameters.pdf

[36] Omeje, C.O. (2020) Corona Loss Minimization on High Voltage Transmission Line Network Using Bundled Conductors. *The International Journal of Engineering and Advanced Technology*, **9**, 887-891. https://doi.org/10.35940/ijeat.C5363.029320

[37] Yaabari, N., Otubu, O.P. and Ojah, O.S. (2021) Impact of High Voltage Transmission on I2R Losses Using a Simplified ETAP Model. *American Journal of Engineering*, **10**, 208-213. https://www.ajer.org/papers/Vol-10-issue-12/U1012208213.pdf

[38] Llamo-Laborí, H.S. and Santos-Fuentefria, A. (2022) A New Method to Calculate Corona Losses for Active Conductors Considering Real Transmission Line Unbalance. *The Journal of Engineering*, **2022**, 725-731. https://doi.org/10.1049/tje2.12155

[39] Ogar, V.N., Bendor, S.A. and James, A.E. (2017) Analysis of Corona Effect on Transmission Line. *American Journal of Engineering Research*, **6**, 75-87. https://www.ajer.org/papers/Vol-10-issue-12/U1012208213.pdf

[40] Al-Issa, H.A., Drechny, M., Trrad, I., *et al.* (2022) Assessment of the Effect of Corona Discharge on Synchronous Generator Self-Excitation. *Energies*, **15**, 2024. https://doi.org/10.3390/en15062024

[41] Al-Hamouz, Z.M. (2019) Corona Power Loss versus Ohmic Power Loss in HYDC Transmission Lines. Department of Electrical Engineering. King Fahd University of Petroleum and Minerals, Dhahran.

[42] Hünnekens, B., Avramidis, G., Ohms, G., *et al.* (2018) Impact of Plasma Treatment under Atmospheric Pressure on Surface Chemistry and Surface Morphology of Extruded and Injection-Molded Wood-Polymer Composites (WPC). *Applied Surface Science*, **441**, 564-574. https://doi.org/10.1016/j.apsusc.2018.01.294

[43] UETCL (2022) Electricity Transmission for Sustainable Regional Development. https://uetcl.go.ug

Appendix

Optimum variables

The optimum variables are obtained by differentiating Equation (4) with respect to these variables, equating the differential to zero and making the optimum variables the subject of the formula in Equations (10)-(12). Thus, differentiating Equation (4) with respect to (wrt) I gives optimum current, I^* Equation (10)

$$\frac{\partial \tilde{p}}{\partial I} = \frac{2I\rho}{A} - \frac{0.0123I\rho\left(V-V_0\right)^2\left(f+25\right)\sqrt{\frac{r}{d}}}{\sqrt{\frac{I^2\rho\left(V-V_0\right)^2\left(f+25\right)\sqrt{\frac{r}{d}}}{A\gamma l}A\gamma l}};$$

$$I^* = \frac{0.00615\sqrt{\sqrt{\frac{r}{d}}d\gamma l\rho Ar\left(f+25\right)\left(V-V_0\right)}}{\sqrt{\frac{r}{d}}d\gamma l\rho} \tag{10}$$

Differentiating Equation (4) wrt transmission phase voltage gives optimum phase transmission voltage, V^* (V) in Equation (11)

$$\frac{\partial \tilde{p}}{\partial V} = \frac{121\left(V-V_0\right)\left(f+25\right)\sqrt{\frac{r}{d}}}{25000\gamma l} - \frac{0.0123I^2\rho\left(V-V_0\right)\left(f+25\right)\sqrt{\frac{r}{d}}}{\sqrt{\frac{I^2\rho\left(V-V_0\right)^2\left(f+25\right)\sqrt{\frac{r}{d}}}{A\gamma l}A\gamma l}};$$

$$V^* = \frac{1}{\sqrt{\frac{r}{d}}A\left(f+25\right)}\left(8.264\times10^{-9}\left(1.21\times10^8 A\sqrt{\frac{r}{d}}fV + 4.84\times10^8 A\sqrt{\frac{r}{d}}V + 3.025\times10^9\sqrt{\frac{r}{d}}AV - 3.0746\times10^8\sqrt{A\sqrt{\frac{r}{d}}f\gamma l\rho I^2 + 25A\sqrt{\frac{r}{d}}\gamma l\rho I^2}\right)\right) \tag{11}$$

Differentiating Equation (4) wrt air density factor gives optimum air density factor, γ^* (kg/m^3) in Equation (12)

$$\frac{\partial \tilde{p}}{\partial \gamma} = -\frac{121\left(V-V_0\right)^2\left(f+25\right)\sqrt{\frac{r}{d}}}{50000l\gamma^2} + \frac{0.00615I^2\rho\left(V-V_0\right)^2\left(f+25\right)\sqrt{\frac{r}{d}}}{\sqrt{\frac{I^2\rho\left(V-V_0\right)^2\left(f+25\right)\sqrt{\frac{r}{d}}}{A\gamma l}A\gamma^2 l}};$$

$$\gamma^* = \frac{0.000759\sqrt{\frac{r}{d}}A\left(V^2 f - 2VfV_0 + fV_0^2 + 25V^2 - 50VV_0 + 25V_0^2\right)}{I^2\rho l} \tag{12}$$

$$H = \begin{bmatrix} \frac{\partial^2(\tilde{p})}{\partial^2 I^2} & \frac{\partial^2(\tilde{p})}{\partial I \partial V} & \frac{\partial^2(\tilde{p})}{\partial I \partial \gamma} \\ \frac{\partial^2(\tilde{p})}{\partial V \partial I} & \frac{\partial^2(\tilde{p})}{\partial^2 V^2} & \frac{\partial^2(\tilde{p})}{\partial V \partial \gamma} \\ \frac{\partial^2(\tilde{p})}{\partial \gamma \partial I} & \frac{\partial^2(\tilde{p})}{\partial \gamma \partial V} & \frac{\partial^2(\tilde{p})}{\partial^2 \gamma^2} \end{bmatrix} \tag{13}$$

Derivatives of the Hessian matrix

The diagonal elements of the Hessian matrix in Equation (13) is given in Equations (14)-(16). The second derivative of power losses, p wrt I is given in Equation (14)

$$\frac{\partial^2 \tilde{p}}{\partial I^2} = \frac{2\rho}{A} + \frac{0.0123 I^2 \rho^2 (V - V_0)^4 (f + 25)^2 \left(\frac{r}{d}\right)}{\left(\frac{I^2 \rho (V - V_0)^2 (f + 25)\sqrt{\frac{r}{d}}}{A\gamma l}\right)^{3/2} A^2 \gamma^2 l^2} - \frac{0.0123 \rho (V - V_0)^2 (f + 25)\sqrt{\frac{r}{d}}}{\sqrt{\frac{I^2 \rho (V - V_0)^2 (f + 25)\sqrt{\frac{r}{d}}}{A\gamma l}} A\gamma l} \tag{14}$$

The second derivative of power losses, p wrt V is given in Equation (15)

$$\frac{\partial^2 \tilde{p}}{\partial V^2} = \frac{121(f + 25)\sqrt{\frac{r}{d}}}{25000\gamma l} + \frac{0.0123 I^4 \rho^2 (V - V_0)^2 (f + 25)^2 \left(\frac{r}{d}\right)}{\left(\frac{I^2 \rho (V - V_0)^2 (f + 25)\sqrt{\frac{r}{d}}}{A\gamma l}\right)^{1.5} A^2 \gamma^2 l^2} - \frac{0.0123 I^2 \rho (f + 25)\sqrt{\frac{r}{d}}}{\sqrt{\frac{I^2 \rho (V - V_0)^2 (f + 25)\sqrt{\frac{r}{d}}}{A\gamma l}} A\gamma l} \tag{15}$$

The second derivative of power losses, p wrt γ is given in Equation (16)

$$\frac{\partial^2 \tilde{p}}{\partial \gamma^2} = \frac{121(V - V_0)^2 (f + 25)\sqrt{\frac{r}{d}}}{25000\gamma^3 l} + \frac{0.00307 I^4 \rho^2 (V - V_0)^4 (f + 25)^2 \left(\frac{r}{d}\right)}{\left(\frac{I^2 \rho (V - V_0)^2 (f + 25)\sqrt{\frac{r}{d}}}{A\gamma l}\right)^{3/2} A^2 \gamma^4 l^2} - \frac{0.0123 I^2 \rho (V - V_0)^2 (f + 25)\sqrt{\frac{r}{d}}}{\sqrt{\frac{I^2 \rho (V - V_0)^2 (f + 25)\sqrt{\frac{r}{d}}}{A\gamma l}} A\gamma^3 l} \tag{16}$$

Upper diagonal elements of Hessian matrix

Upper diagonal elements are derived in Equations (17)-(19). The second derivative of power losses wrt I and V is given in Equation (17)

$$\frac{\partial^2 \tilde{p}}{\partial I \partial V} = \frac{0.0123 I^3 \rho^2 \left(V - V_0\right)^3 \left(f + 25\right)^2 \left(\frac{r}{d}\right)}{\left(\frac{I^2 \rho \left(V - V_0\right)^2 \left(f + 25\right) \sqrt{\frac{r}{d}}}{Al\gamma}\right)^{1.5} A^2 \gamma^2 l^2} - \frac{0.0246 I \rho \left(V - V_0\right)\left(f + 25\right) \sqrt{\frac{r}{d}}}{\sqrt{\frac{I^2 \rho \left(V - V_0\right)^2 \left(f + 25\right) \sqrt{\frac{r}{d}}}{Al\gamma}} A\gamma l} \tag{17}$$

The second derivative of power losses wrt I and γ is given in Equation (18)

$$\frac{\partial^2 \tilde{p}}{\partial I \partial \gamma} = -\frac{0.00615 I^3 \rho^2 \left(V - V_0\right)^4 \left(f + 25\right)^2 \left(\frac{r}{d}\right)}{\left(\frac{I^2 \rho \left(V - V_0\right)^2 \left(f + 25\right) \sqrt{\frac{r}{d}}}{Al\gamma}\right)^{1.5} A^2 \gamma^3 l^2} + \frac{0.0123 \rho \left(V - V_0\right)^2 \left(f + 25\right) \sqrt{\frac{r}{d}}}{\sqrt{\frac{I^2 \rho \left(V - V_0\right)^2 \left(f + 25\right) \sqrt{\frac{r}{d}}}{A\gamma l}} A\gamma^2 l} \tag{18}$$

The second derivative of power losses w.r.t V and γ is given in Equation (19)

$$\frac{\partial^2 \tilde{p}}{\partial V \partial \gamma} = -\frac{121 \left(V - V_0\right) \sqrt{\frac{r}{d}}}{25000 l \gamma^2} - \frac{0.00615 I^4 \rho^2 \left(V - V_0\right)^3 \left(f + 25\right)^2 \left(\frac{r}{d}\right)}{\left(\frac{I^2 \rho \left(V - V_0\right)^2 \left(f + 25\right) \sqrt{\frac{r}{d}}}{Al\gamma}\right)^{1.5} A^2 \gamma^3 l^2} + \frac{0.0123 I^2 \rho \left(V - V_0\right)\left(f + 25\right) \sqrt{\frac{r}{d}}}{\sqrt{\frac{I^2 \rho \left(V - V_0\right)^2 \left(f + 25\right) \sqrt{\frac{r}{d}}}{A\gamma l}} A\gamma^2 l} \tag{19}$$

Lower diagonal elements of Hessian matrix

The lower diagonal elements of the Hessian matrix are obtained as the reciprocal of Equations (20)-(22).

The second derivative of power losses wrt V and I is given in Equation (20)

$$\frac{\partial^2 \tilde{p}}{\partial V \partial I} = \frac{0.0123 I^3 \rho^2 (V - V_0)^3 (f + 25)^2 \left(\frac{r}{d}\right)}{\left(\frac{I^2 \rho (V - V_0)^2 (f + 25) \sqrt{\frac{r}{d}}}{Al\gamma}\right)^{1.5} A^2 \gamma^2 l^2} - \frac{0.0246 I \rho (V - V_0)(f + 25) \sqrt{\frac{r}{d}}}{\sqrt{\frac{I^2 \rho (V - V_0)^2 (f + 25) \sqrt{\frac{r}{d}}}{Al\gamma}} A\gamma l} \tag{20}$$

The second derivative of power losses wrt γ and I is given in Equation (21)

$$\frac{\partial^2 \tilde{p}}{\partial \gamma \partial I} = -\frac{0.00615 I^3 \rho^2 (V - V_0)^4 (f + 25)^2 \left(\frac{r}{d}\right)}{\left(\frac{I^2 \rho (V - V_0)^2 (f + 25) \sqrt{\frac{r}{d}}}{Al\gamma}\right)^{1.5} A^2 \gamma^3 l^2} + \frac{0.0123 I \rho (V - V_0)^2 (f + 25) \sqrt{\frac{r}{d}}}{\sqrt{\frac{I^2 \rho (V - V_0)^2 (f + 25) \sqrt{\frac{r}{d}}}{A\gamma l}} A\gamma^2 l} \tag{21}$$

The second derivative of power losses wrt γ and V is given in Equation (22)

$$\frac{\partial^2 \tilde{p}}{\partial \gamma \partial V} = -\frac{121 (V - V_0) \sqrt{\frac{r}{d}}}{25000 l \gamma^2} - \frac{0.00615 I^4 \rho^2 (V - V_0)^3 (f + 25)^2 \left(\frac{r}{d}\right)}{\left(\frac{I^2 \rho (V - V_0)^2 (f + 25) \sqrt{\frac{r}{d}}}{Al\gamma}\right)^{1.5} A^2 \gamma^3 l^2} + \frac{0.0123 I^2 \rho (V - V_0)(f + 25) \sqrt{\frac{r}{d}}}{\sqrt{\frac{I^2 \rho (V - V_0)^2 (f + 25) \sqrt{\frac{r}{d}}}{A\gamma l}} A\gamma^2 l} \tag{22}$$